Multiple Supercritical Solitary Wave Solutions of the Stationary Forced Korteweg-De Vries Equation and their Stability
Author(s): Lianger Gong and Samuel S. Shen
Source: *SIAM Journal on Applied Mathematics*, Vol. 54, No. 5 (Oct., 1994), pp. 1268-1290
Published by: Society for Industrial and Applied Mathematics
Stable URL: http://www.jstor.org/stable/2102469
Accessed: 19/07/2010 14:08

Your use of the JSTOR archive indicates your acceptance of JSTOR's Terms and Conditions of Use, available at http://www.jstor.org/page/info/about/policies/terms.jsp. JSTOR's Terms and Conditions of Use provides, in part, that unless you have obtained prior permission, you may not download an entire issue of a journal or multiple copies of articles, and you may use content in the JSTOR archive only for your personal, non-commercial use.

Please contact the publisher regarding any further use of this work. Publisher contact information may be obtained at http://www.jstor.org/action/showPublisher?publisherCode=siam.

Each copy of any part of a JSTOR transmission must contain the same copyright notice that appears on the screen or printed page of such transmission.

JSTOR is a not-for-profit service that helps scholars, researchers, and students discover, use, and build upon a wide range of content in a trusted digital archive. We use information technology and tools to increase productivity and facilitate new forms of scholarship. For more information about JSTOR, please contact support@jstor.org.

Society for Industrial and Applied Mathematics is collaborating with JSTOR to digitize, preserve and extend access to *SIAM Journal on Applied Mathematics.*

http://www.jstor.org

SIAM J. APPL. MATH.
Vol. 54, No. 5, pp. 1268–1290, October 1994
© 1994 Society for Industrial and Applied Mathematics
006

MULTIPLE SUPERCRITICAL SOLITARY WAVE SOLUTIONS OF THE STATIONARY FORCED KORTEWEG–DE VRIES EQUATION AND THEIR STABILITY*

LIANGER GONG† AND SAMUEL S. SHEN‡

Abstract. The first-order approximation of long nonlinear surface waves in a channel flow of an inviscid, incompressible fluid over a bump results in a forced Korteweg–de Vries equation (fKdV):

$$\eta_t + \lambda\eta_x + 2\alpha\eta\eta_x + \beta\eta_{xxx} = f_x(x), \quad -\infty < x < \infty, \quad t > 0.$$

The forcing represented by the function $f(x)$ in the fKdV equation is due to the bump on the bottom of the channel. In this paper, the solitary wave solutions of the stationary fKdV equation (sfKdV) are studied. The supercritical solitary wave solutions of the sfKdV equation exist only when the upstream flow velocity c^* is greater than a crucial value $u_c > \sqrt{gH}$, or equivalently, $\lambda > \lambda_c > 0$. The existence of supercritical positive solitary wave solutions (SPSWS) of the sfKdV equation is proved. Some ordered properties and extreme properties of SPSWS are discussed. There may exist more than two SPSWS for a nonlocal forcing. An analytic expression of the SPSWS is found when the forcing is a rectangular bump or dent (called the well-shape forcing). Analytic solutions explicitly reveal the multiplicity of solutions and make the complicated sfKdV bifurcation behavior more transparent. Multiple SPSWS are also found numerically when the forcing is a partly negative and partly positive bump, and two semi-elliptic bumps, respectively. Numerical simulations show that only one of the four SPSWS for a well-shape forcing is stable.

Key words. forced Korteweg–de Vries equation, solitary waves, multiple solutions, stability

AMS subject classifications. 76B15, 34B15, 35Q53

1. Introduction. Six years ago, Vanden-Broeck [11] considered the time-independent surface waves of an incompressible and inviscid fluid flow over a bump in a two-dimensional channel. The bottom of the channel has a semicircular bump and is otherwise flat. Both the upstream flow and the downstream flow are uniform with velocity c^* and depth H. The upstream Froude number F, which is defined as the ratio of the upstream velocity to the critical speed of shallow water waves $\sqrt{gH}$, is greater than one. He used the conformal mapping and Cauchy integration techniques to convert the Laplace equation in the fluid domain with nonlinear boundary conditions on the free surface into an integral equation of a complex variable. This integral equation was then solved numerically. This method was first derived by Forbes and Schwartz for the same fluid flow problem [4]. Vanden-Broeck's significant contribution to this problem is the discovery of the existence of two branches of supercritical positive solitary wave solutions (SPSWS). Here, "supercritical" means that $F \geq F_C > 1$ where F_C is determined by the size of the bump. "Positive" means that the free surface elevation $\eta(x) > 0$ for any finite $x \in \Re$. And "solitary wave" means that the free surface elevation η has the property: $\eta(\pm\infty) = \eta_x(\pm\infty) = \eta_{xx}(\pm\infty) = 0$. Vanden-Broeck's computational results showed that when the Froude number F increases or the bump size approaches zero, the upper branch of the solutions approaches the solitary wave in a flat channel and the lower branch approaches the uniform

* Received by the editors June 30, 1992; accepted for publication (in revised form) October 20, 1993.

† Department of Mathematics, University of Alberta, Edmonton, Alberta, Canada T6G 2G1. This author's research was supported in part by the Graduate Fellowship of the University of Saskatchewan from 1990 to 1991.

‡ Department of Mathematics, University of Alberta, Edmonton, Alberta, Canada T6G 2G1. This author's research was supported in part by Natural Sciences and Engineering Research Council of Canada grant OGP IN 016.

flow (i.e., the null solution). Forbes and Schwartz's findings are the solutions of the lower branch.

Two years later, Shen [8] published his findings on the similar bifurcation phenomenon from the time independent forced Korteweg–de Vries equation (sfKdV). The equation is of the following form:

$$\lambda\eta_x + 2\alpha\eta\eta_x + \beta\eta_{xxx} = f_x(x), \qquad -\infty < x < \infty \tag{1}$$

with the solitary wave boundary conditions

$$\eta(\pm\infty) = \eta_x(\pm\infty) = \eta_{xx}(\pm\infty) = 0. \tag{2}$$

Here, $\lambda > 0$ (means supercritical), $\alpha < 0$ and $\beta < 0$ are constants. Shen's results obtained from this simple BVP of an ordinary differential equation qualitatively agree with Vanden-Broeck's. Namely, when λ is sufficiently large, there exist two branches of SPSWS: $\eta_u(x)$ and $\eta_\ell(x)$ with the following properties:

$$\eta_u(x) \sim -\frac{3\lambda}{2\alpha}\operatorname{sech}^2\left(\sqrt{\frac{-\lambda}{4\beta}}(x - x_0)\right),$$

$$\eta_\ell(x) \sim 0$$

as $\lambda \to \infty$. In a two-dimensional channel, $F = 1 + \epsilon\lambda$ and ϵ is a small positive constant. Therefore, $\lambda \to \infty$ implies that $F \to \infty$, the limit described by Vanden-Broeck (cf. [11]).

The sfKdV equation (1) was derived for the small elevation of the free surface of order ϵH and for a small amplitude forcing of order $\epsilon^2 H$, whereas Vanden-Broeack's model was for finite amplitude waves and a large bump (the bump height R is as large as a half of the depth H of the upstream fluid). Hence, it was generally consented that Vanden-Broeck [11] and Shen [8] were studying different classes of models: Vanden-Broeck for large bumps and the finite elevation of the free surface, and Shen for small bumps and the small elevation of the free surface. Only until recently, Shen surprisingly found that the valid range of the simple sfKdV equation is not restricted to small bumps and small elevations [10]. Rather, with little error, it is a valid approximation model equation for all cases when Vanden-Broeck's computational scheme converges and when experiments can be conducted. Namely, the sfKdV equation is a valid approximation model as long as the corresponding physics exists.

Since the sfKdV equation is the result of the first order approximation, an error usually exists when using the sfKdV equation as a model equation to quantitatively describe the wave physics. This error should be of order ϵ^2 and hence varies according to the "small" dimensionless number "ϵ". This "small" dimensionless number "ϵ" is determined by the size of the bump and measures the nonlinearity and dispersion, and is used as an ordering scale in the formal asymptotic approximation. Shen's startling findings showed that the error is still within 10% when the "small" number ϵ is as large as 0.7. When $\epsilon = 0.7$, the sfKdV equation models the same physics as that studied by Vanden-Broeck for $\alpha = R/H = 0.5$, where R is the radius of the circular bump. Shen's investigation has provided sufficient evidence that the sfKdV equation is a parsimonious asymptotic model for the corresponding physics. Here, "parsimonious" is a word adopted from Ludwig's paper [5] and means "simple" and "correct" in the sense of small error.

In the sfKdV equation, the forcing is usually classified into two types. One type of the forcing called "local" forcing, whose height is comparable with the length of the

base support, can be approximated by the Dirac delta function in the dimensionless long wave coordinates. In Shen's 1992 paper [10], considered was basically this type of the forcing. All the solutions of the sfKdV equation can be found analytically. The other type of forcing is called "nonlocal" forcing. In the laboratory coordinates, it means that the support of the bump is much longer than the height of the bump. In particular, the bump length under our consideration is comparable with the length scale of the free surface wave. The sfKdV equation with nonlocal forcing has some different properties from that with local forcing. For instance, the sfKdV equation may admit more than two SPSWS when the forcing is nonlocal and negative. This is in sharp contrast to the fact that the locally sfKdV equation have at most two SPSWS. In this study, our focus is on the multiple SPSWS of the sfKdV equation with nonlocal forcing and their stability. The following results constitute the novel features of this paper:

(i) Proof of the positivity of solitary wave solutions of the sfKdV equation;

(ii) Some ordered properties and extreme properties of the SPSWS;

(iii) Analytic expressions of the SPSWS when the forcing is a rectangular bump or dent;

(iv) Numerical SPSWS and their bifurcation when the forcing is a partly negative and partly positive bump, and two semi-elliptic bumps, respectively;

(v) Numerical simulations on the instability of the SPSWS.

The proof of the existence of the SPSWS, although not completely new, fills up a gap in Shen's earlier proof (cf. [8]). The ordered properties and extreme properties are useful in understanding the differences among multiple SPSWS and envisaging the bifurcation behavior of the boundary value problem for the sfKdV equation. These properties, some of which are sharp, have not appeared in literature before. Analytic solutions explicitly reveal the multiplicity of the solutions and make the complicated sfKdV bifurcation behavior more transparent. Although the analytic solutions are constructed for the particular rectangular forcing, some of their properties which depend only on the area of the forcing (i.e., $\int_{-\infty}^{\infty} f(x)\ dx$) are applicable to the forcing of other shapes. Numerical solutions are necessary for most types of forcing. The most subtle point in searching for multiple solutions is the transition from 2 solutions to 4 solutions, from 4 solutions to 6 solutions, and so on. The stability of an SPSWS is defined according to the evolution of this solution with respect to the time dependent fKdV equation. Our study is based on numerical simulations and the small perturbation to the original SPSWS is introduced through truncation errors (or called numerical noise) in numerical calculation. Our numerical results show that only one SPSWS is stable and the co-existence of two or more stable states does not appear although it is common in biological and chemical models. To the authors' knowledge, all these conclusions are new to the existing literature.

We have arranged the context of this paper as follows. To make the paper self-contained, we recapitulate the derivation of the sfKdV equation in §2. Analytical properties are studied in §3. These include the existence of the SPSWS, some ordered and extreme properties of the SPSWS. A well-shape forcing is considered in §4. An analytic expression of the SPSWS is found in term of the Weierstrass elliptic function. Numerical SPSWS for different types of forcing are presented in §5. Numerical simulations on the instability of the SPSWS are carried out in §6. In §7, we make some concluding remarks.

2. Derivation of the sfKdV equation. The fluid under consideration is inviscid and incompressible. The fluid flow configuration is shown in Fig. 1. Let the

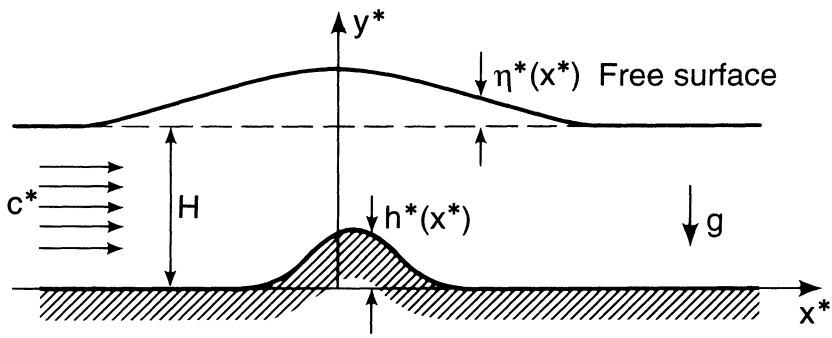

FIG. 1. *Configuration of a single-layer fluid flow forced by a bump on the bottom of a two-dimensional channel.*

x^*-axis be aligned along the longitudinal direction and on the bottom of the channel, and the y^*-axis vertically opposite to the gravitational direction. Let H be the upstream depth of the fluid, ρ the density, p^* the pressure, (u^*, v^*) the velocity, η^* the free-surface elevation, c^* the upstream uniform velocity, $y^* = h^*(x^*)$ the bottom topography and g is the gravitational acceleration.

Let L be the typical wave length. We use L, H and ρ as the horizontal length scale, the vertical length scale and the density scale, respectively. The following dimensionless variables are introduced:

$$\epsilon = (H/L)^2 \ll 1 \quad \text{(the small parameter in the sfKdV asymptotic analysis)},$$

$$(x, y) = (\epsilon^{1/2} x^*, y^*)/H, \qquad \psi = \psi^*/(c^* H),$$

$$p = p^*/(\rho g H), \qquad (u, v) = (u^*, \epsilon^{-1/2} v^*)/\sqrt{gH},$$

$$F = c^*/\sqrt{gH} \quad \text{(Froude number)}, \qquad \eta = \eta^*/H,$$

$$h(x) = \epsilon^{-2} h^*(x^*)/H \quad \text{(the small bump assumption)}.$$

Since the flow is laminar, both the free-surface and the bottom of the channel are stream lines. Let ψ be the dimensionless stream function such that $\psi = 1$ on the free-surface and $\psi = 0$ on the bottom. Then

$$u = F\frac{\partial \psi}{\partial y}, \qquad v = -F\frac{\partial \psi}{\partial x}.$$

We make the following coordinate transformation: $(x, y) \longrightarrow (\zeta, \psi)$ such that $\zeta = x, \psi = \psi(x, y)$. Hence $(\zeta = x, \psi = \psi(x, y))$ maps the fluid domain in the x, y-plane onto a strip $\Omega = \Re \times (0, 1)$ in the ζ, ψ-plane. Here (ζ, ψ) is called the streamline coordinate system. Let $(x = \zeta, y = f(\zeta, \psi))$ be the inverse transformation of $(x, y) \longrightarrow (\zeta, \psi)$. In terms of the streamline coordinates (ζ, ψ), we have

$$u = \frac{F}{f_\psi}, \qquad v = F\frac{f_\zeta}{f_\psi}, \qquad \frac{\partial}{\partial x} = \frac{\partial}{\partial \zeta} - \frac{v}{F}\frac{\partial}{\partial \psi}, \qquad \frac{\partial}{\partial y} = \frac{u}{F}\frac{\partial}{\partial \psi}.$$

From the irrotational property of the flow, one can derive a second-order partial differential equation for f with independent variables ζ and ψ in Ω. Since the stream function is used, the kinematic boundary conditions on both the free-surface and the

bottom are satisfied automatically. Hence, the Bernoulli equation shall serve as the boundary condition on $\psi = 1$, and the bottom topography shall serve as the boundary condition on $\psi = 0$. The resulting boundary value problem is posed by

$$\epsilon f_\psi^2 f_{\zeta\zeta} - 2\epsilon f_\zeta f_\psi f_{\zeta\psi} + (1 + \epsilon f_\zeta^2) f_{\psi\psi} = 0 \quad \text{in } \Omega, \tag{3}$$

$$F^2(1 + \epsilon f_\zeta^2) + \left[2(f-1) - F^2\right] f_\psi^2 = 0 \quad \text{on } \psi = 1, \tag{4}$$

$$f = \epsilon^2 h(\zeta) \quad \text{on } \psi = 0. \tag{5}$$

The above procedure was used back in 1960 by Peters and Stoker [7].

Let F_0 be the critical Froude number. It is assumed that the upstream velocity is near the critical speed and the response of the free-surface elevation to the bump is of order $O(\epsilon)$. Hence we have the following asymptotic expansion:

$$f = \psi + \epsilon f_1(\zeta, \psi) + \epsilon^2 f_2(\zeta, \psi) + O(\epsilon^3), \tag{6}$$

$$F = F_0 + \epsilon\lambda + O(\epsilon^2). \tag{7}$$

Substituting (6)–(7) into (3)–(5), one can obtain a sequence of equations of successive orders. We need to use only those equations of the first two orders.

The equations of the first order (i.e., $O(\epsilon)$ order) imply that

$$f_1 = \psi A(\zeta), \quad F_0^2 = 1 \ \text{(the critical speed of the shallow water waves)},$$

where A is an arbitrary function of ζ to be determined by the solvability condition of the second order (i.e., $O(\epsilon^2)$ order) problem. Since $f_1(\zeta, \psi = 1) = A(\zeta = x)$, the function $A(x)$ is actually the profile of the first order elevation of the free-surface and satisfies the equation

$$A'' - 6\lambda A = -\frac{9}{2}A^2 - 3h.$$

This is the first integral of the stationary fKdV problem (1)–(2) when $\alpha = -3/4$, $\beta = -1/6$, $f(x) = h(x)/2$, and $A(x) = \eta(x)$.

3. Analytical properties of the SPSWS. In this section, we assume that $\lambda > 0$, $\alpha < 0$, $\beta < 0$, and $f(x) \in C_0^1(\Re)$. Shen proved that the BVP (1)–(2) for $f(x) \geq 0$ has at least one solution if λ is sufficiently large [8]. Also, he claimed that every solution is positive. Namely, every solution is an SPSWS. However, there was a gap in Shen's proof of this positivity claim. Here, we provide a complete proof that fills up the gap.

THEOREM 3.1 (positivity property). *Suppose that $\eta(x)$ is a solution of the following* BVP:

$$\lambda\eta + \alpha\eta^2 + \beta\eta'' = f(x), \qquad -\infty < x < +\infty, \tag{8}$$

$$\eta(\pm\infty) = \eta'(\pm\infty) = 0, \tag{9}$$

where $\lambda > 0$, $\alpha < 0$, $\beta < 0$, $f(x) \geq 0$ and $f(x) \in C_0^1(\Re)$, then $\eta(x) > 0$ for any $x \in \Re$.

Proof. If $\eta(x)$ is a solution of the BVP (8)–(9), then we have

$$\eta(x) = \frac{1}{\beta}\int_{-\infty}^{+\infty} K(x, \xi)\left(\alpha\eta^2(\xi) - f(\xi)\right) d\xi, \tag{10}$$

where $K(x,\xi) = \frac{1}{2\nu}\exp(-\nu|\xi - x|)$ is the Green's function satisfying

$$\begin{cases} K_{\xi\xi} - \nu^2 K = -\delta(\xi - x), \\ K(\xi = \pm\infty, x) = 0, \qquad \nu = \sqrt{-\lambda/\beta}. \end{cases}$$

Clearly, $\eta(x) \geq 0$ holds for any $x \in \Re$ since $\alpha < 0$, $\beta < 0$, $K(x,\xi) \geq 0$ and $f(\xi) \geq 0$ for any $\xi \in \Re$.

Now, suppose that there exists a point $a \in \Re$ such that $\eta(a) = 0$. From (10),

$$\eta(a) = \frac{1}{\beta}\int_{-\infty}^{+\infty} K(a,\xi)\left(\alpha\eta^2(\xi) - f(\xi)\right) d\xi = 0.$$

Since $K(a,\xi) > 0$ and $\alpha\eta^2(\xi) - f(\xi) \leq 0$ we have $\alpha\eta^2(\xi) = f(\xi)$ for any $\xi \in \Re$. This is a contradiction since $f(\xi_1) > 0$ for some $\xi_1 \in \Re$ whereas $\alpha\eta^2(\xi_1)$ is always less or equal to zero. Hence, $\eta(x) > 0$ for any $x \in \Re$. □

After resolving the existence question of the SPSWS, let us discuss various properties of the SPSWS. For multiple solutions, it is interesting to investigate the relative position of the solutions. When we say that two solutions $\eta_1(x)$ and $\eta_2(x)$ of the BVP (8)–(9) are ordered, we mean that $\eta_1(x) \neq \eta_2(x)$ for any $x \in \Re$. Numerous numerical solutions we obtained seem to suggest that if there exists a third solution of the BVP (8)–(9), then it cannot be ordered with other already ordered solutions. Indeed, this is generally true. We have found that the SPSWS of the BVP (8)–(9) have the following ordered properties.

THEOREM 3.2 (ordered properties). (i) *The* BVP (8)–(9) *admits at most two ordered* SPSWS; (ii) *If two distinct solutions* $\eta_1(x)$ *and* $\eta_2(x)$ *of the* BVP (8)–(9) *satisfy* $\| \eta_1 \|_\infty > \| \eta_2 \|_\infty$ *and* $\| \eta_2 \|_\infty \leq -\frac{\lambda}{2\alpha}$, *then* $\eta_1(x) > \eta_2(x)$ *for each* $x \in \Re$.

Proof. (i) If the theorem were not true, the BVP (8)–(9) would admit at least three ordered SPSWS. Assume that η_i $(i = 1,2,3)$ are three ordered solutions and, without loss of generality, $0 < \eta_1 < \eta_2 < \eta_3$. Let $w_1 = \eta_2 - \eta_1$, and $w_2 = \eta_3 - \eta_2$. From (8), it follows that

$$\beta w_1'' = [-\lambda - \alpha(\eta_1 + \eta_2)]w_1, \tag{11}$$

$$\beta w_2'' = [-\lambda - \alpha(\eta_2 + \eta_3)]w_2. \tag{12}$$

Multiplying (11) by w_2 and (12) by $-w_1$, adding the two resulting equations together and integrating the sum from $-\infty$ to ∞, we have

$$\int_{-\infty}^{\infty} (w_1 + w_2)w_1 w_2\, dx = 0.$$

Clearly, w_1 and w_2 are positive for any $x \in \Re$. This is a contradiction and the proof of (i) is finished.

Hence, if there exists a third SPSWS of the BVP (8)–(9), then it cannot be ordered with the other two.

(ii) The second ordered property is based on the following two facts. First, under the assumptions of (ii), $\eta_1(x) \geq \eta_2(x)$ for any $x \in \Re$. If this were not true, there would exist $x_0 \in \Re$ such that $\eta_1(x_0) < \eta_2(x_0)$. Let $w(x) = \eta_1(x) - \eta_2(x)$. Then, putting $\eta_1(x) = w(x) + \eta_2(x)$ into (8), one gets

$$(\lambda + 2\alpha\eta_2(x))\, w(x) + \alpha w^2(x) + \beta w''(x) = 0, \qquad x \in \Re. \tag{13}$$

On the other hand, the function $w(x)$ has at least a local minimum point a such that $w(a) < 0$ and $w''(a) \geq 0$ since $w(x_0) < 0$ and $w(\pm\infty) = 0$. Also, by the assumption (ii) $\lambda + 2\alpha\eta_2(a) \geq 0$, we have

$$(\lambda + 2\alpha\eta_2(a))\, w(a) + \alpha w^2(a) + \beta w''(a) < 0.$$

This contradicts (13). Hence, $\eta_1(x) \geq \eta_2(x)$ for any $x \in \Re$.

The second fact is, according to the theory of ordinary differential equations, that the IVP

$$(\lambda + 2\alpha\eta_2(x))\, w(x) + \alpha w^2(x) + \beta w''(x) = 0, \qquad x \in \Re, \tag{14}$$

$$w(x_0) = w'(x_0) = 0, \qquad x_0 \in \Re, \tag{15}$$

has only a trivial solution when $\eta_2(x)$ is a given bounded function. In fact, (14)–(15) can be viewed as a system of the first-order differential equations:

$$\frac{dw}{dx} = v, \tag{16}$$

$$\frac{dv}{dx} = -\frac{1}{\beta}\left[(\lambda + 2\alpha\eta_2)w + \alpha w^2\right], \tag{17}$$

with initial value conditions: $w(x_0) = 0$ and $v(x_0) = 0$.

Since the right-hand side of (16)–(17) is obviously in C^1 and hence satisfies Lipschitz condition, the IVP (16)–(17) has only a trivial solution, that is, $w(x) = 0$ for any $x \in \Re$.

Now, let us return to the proof of the claim (ii). Suppose that the conclusion fails to hold. There must exist $x_0 \in \Re$ such that $\eta_1(x_0) = \eta_2(x_0)$, i.e., $w(x_0) = 0$. By the first fact, x_0 is a minimum point of $w(x)$, hence, $w'(x_0) = 0$. Then, by the second fact, $\eta_1(x) = \eta_2(x)$ for any $x \in \Re$. This is a contradiction to the assumption and completes our proof. □

It is clear that every solution to the BVP (8)–(9) is bounded. Finally, our concerns are on the extreme properties of solutions of the BVP (8)–(9).

THEOREM 3.3 (extreme properties). (i) *If $\eta(x)$ is a solution of the* BVP (8)–(9) *and $f(x) \in C_0^1(\Re)$, then either*

$$\| \eta \|_\infty \leq \frac{\sqrt{\lambda^2 + 4\alpha \| f \|_\infty} - \lambda}{2\alpha} \quad \text{or} \quad \| \eta \|_\infty \geq -\frac{\sqrt{\lambda^2 + 4\alpha \| f \|_\infty} + \lambda}{2\alpha}, \tag{18}$$

where $\| f \|_\infty = \max\{|f(x)|, x \in \Re\}$; (ii) *if $\eta(x)$ is an* SPSWS *of the* BVP (8)–(9) *and $f(x) \leq 0$, then $\| \eta \|_\infty \geq -\lambda/\alpha$*; (iii) *if $\eta(x)$ is an* SPSWS *of the* BVP (8)–(9) *and $f(x) \geq 0$ and x_0 is a local minimum point of $\eta(x)$ in $\Re$, then $\eta(x_0) \leq -\lambda/\alpha$*; (iv) *if $\eta(x)$ is an* SPSWS *of the* BVP (8)–(9), *and if $\eta(x) \geq -\lambda/\alpha$ and $f(x) \geq 0$ for all $x \in \operatorname{supp}(f)$, then $\eta(x)$ has at most one local extreme point in* $\operatorname{supp}(f)$.

Proof. (i) By (10), one can get

$$|\eta(x)| \leq \frac{1}{|\beta|}(|\alpha| \| \eta \|_\infty^2 + \| f \|_\infty) \int_{-\infty}^{+\infty} K(x, \xi) d\xi.$$

Direct calculation of the aboye integral yields

$$\int_{-\infty}^{+\infty} K(x, \xi) d\xi = |\beta|/\lambda.$$

Thus

$$|\alpha| \parallel \eta \parallel_\infty^2 - \lambda \parallel \eta \parallel_\infty + \parallel f \parallel_\infty \geq 0,$$

which is equivalent to (18).

(ii) By the continuity of $\eta(x)$, there exists $x_0 \in \Re$ such that $\eta(x_0) = \parallel \eta \parallel_\infty$, $\eta'(x_0) = 0$, and $\eta''(x_0) \leq 0$. Since $f(x) \leq 0$, from (8), we have

$$\lambda\eta(x_0) + \alpha\eta^2(x_0) = f(x_0) - \beta\eta''(x_0) \leq 0.$$

The condition $\eta(x_0) > 0$ implies that $\lambda + \alpha\eta(x_0) \leq 0$. Therefore, $\parallel \eta \parallel_\infty = \eta(x_0) \geq -\lambda/\alpha$.

(iii) Since x_0 is a local minimum point of $\eta(x)$, then $\eta'(x_0) = 0$, and $\eta''(x_0) \geq 0$. By (8), the condition $f(x) \geq 0$ implies

$$\lambda\eta(x_0) + \alpha\eta^2(x_0) = f(x_0) - \beta\eta''(x_0) \geq 0.$$

Hence, from $\eta(x_0) > 0$, we have $\lambda + \alpha\eta(x_0) \geq 0$, i.e., $\eta(x_0) \leq -\lambda/\alpha$.

(iv) Suppose that $\eta(x)$ has two local extreme points a and b with $a < b$ in $\text{supp}(f)$, then $\eta'(a) = \eta'(b) = 0$. Integrating (8) with respect to x from a to b yields

$$\int_a^b \left[\lambda\eta(x) + \alpha\eta^2(x)\right] dx + \beta\left[\eta'(b) - \eta'(a)\right] = \int_a^b f(x)dx.$$

This implies that

$$\int_a^b \left[\lambda\eta(x) + \alpha\eta^2(x)\right] dx > 0 \tag{19}$$

since $f(x) > 0$ for any $x \in [a, b] \subset \text{supp}(f)$. On the other hand, the assumption $\eta(x) \geq -\lambda/\alpha > 0$ for all $x \in \text{supp}(f)$ leads to

$$\int_a^b \left[\lambda\eta(x) + \alpha\eta^2(x)\right] dx \leq 0.$$

This contradicts (19), and our proof is completed. □

4. Analytic expression of the SPSWS. It is interesting to solve the BVP (8)–(9) analytically. Patoine and Warn [6], Shen [9], and Wu [13] have found analytic expressions for the solutions of the BVP (8)–(9) with different types of forcing functions. In this section, we show that the solitary wave solutions of the BVP (8)–(9) for a nonlocal well-shape forcing

$$f(x) = \begin{cases} -1, & |x| \leq a/2, \\ 0, & \text{otherwise} \end{cases}$$

can be expressed in terms of Weierstrass' elliptic functions in the region of the rectangular dent and matched by hyperbolic sech^2-type of functions outside of the dent. Here a is a positive constant which represents the length of the rectangular dent.

4.1. Analytic expression of the SPSWS. Since the forcing function $f(x)$ has a jump discontinuity, the SPSWS $\eta(x)$ of the BVP (8)–(9) are all in $C^1(\Re)$. When $x \leq -a/2$, the SPSWS $\eta(x)$ of the BVP(8)–(9) can be expressed by

$$\eta(x) = -\frac{3\lambda}{2\alpha}\operatorname{sech}^2\sqrt{\frac{-\lambda}{4\beta}}(x - L_0),$$

where the phase shift L_0 is to be determined.

When $|x| < a/2$, the SPSWS $\eta(x)$ must satisfy the equation

$$\lambda\eta + \alpha\eta^2 + \beta\eta'' = -1. \tag{20}$$

The continuity of η and η' at $x = -a/2$ and $x = a/2$ yields

$$\eta(-a/2) = -\frac{3\lambda}{2\alpha}\operatorname{sech}^2\sqrt{\frac{-\lambda}{4\beta}}(a/2 + L_0) \equiv \eta_0, \tag{21}$$

$$\eta'(-a/2) = \sqrt{\frac{-\lambda}{\beta}}\eta_0 \tanh\sqrt{\frac{-\lambda}{4\beta}}(a/2 + L_0) \equiv \eta_1, \tag{22}$$

$$\eta(-a/2) = \eta(a/2), \tag{23}$$

$$\eta'(-a/2) = \eta'(a/2), \quad \text{or} \quad \eta'(-a/2) = -\eta'(a/2). \tag{24}$$

The first integral of (20) from $-a/2$ to x $(< a/2)$ satisfies

$$(\eta')^2 = b_1\eta^3 + b_2\eta^2 + b_3\eta + b_4, \tag{25}$$

where $b_1 = -(2\alpha)/(3\beta), b_2 = -\lambda/\beta, b_3 = -2/\beta$, and $b_4 = -b_3\eta_0$. By making a transform $\eta = c_1u + c_2$, (25) is converted into

$$(u')^2 = 4u^3 - g_2u - g_3, \tag{26}$$

where $c_1 = 4/b_1, c_2 = -b_2/(3b_1), g_2 = -(b_2c_2 + b_3)/c_1$, and $g_3 = -(b_1c_2^3 + b_2c_2^2 + b_3c_2 + b_4)/c_1^2$. Here, g_2 is a constant and g_3 is a function of L_0 for given λ, α, β, and a. The general solution of (26) can be expressed in term of Weierstrass' elliptic function $u = \wp(x + \tau, g_2, g_3)$ (cf. [12, p. 470]). Thus, when $|x| < a/2$, the SPSWS $\eta(x)$ can be written as

$$\eta(x) = c_1\wp(x + \tau, g_2, g_3) + c_2. \tag{27}$$

Equations (21) and (22) are reduced to

$$\eta_0 = c_1\wp(-a/2 + \tau, g_2, g_3) + c_2, \tag{28}$$

$$\eta_1 = c_1\wp'(-a/2 + \tau, g_2, g_3). \tag{29}$$

Further, from the following identity of Weierstrass' elliptic function (cf. [12, p. 482])

$$\wp(x + y, g_2, g_3) + \wp(x, g_2, g_3) + \wp(y, g_2, g_3) = \frac{1}{4}\left\{\frac{\wp'(x, g_2, g_3) - \wp'(y, g_2, g_3)}{\wp(x, g_2, g_3) - \wp(y, g_2, g_3)}\right\}^2,$$

Weierstrass' elliptic function $\wp(x+\tau, g_2, g_3)$ in (27) can be rewritten in the following form:

$$\wp(x+\tau, g_2, g_3) = \frac{1}{4}\left\{\frac{c_1\wp'(x+a/2, g_2, g_3) - \eta_1}{c_1\wp(x+a/2, g_2, g_3) - \eta_0 + c_2}\right\}^2 - \wp(x+a/2, g_2, g_3) - \frac{\eta_0 - c_2}{c_1}.$$

Equation (23) yields another equation:

$$(30)\quad B(\lambda, L_0) \equiv \frac{c_1}{4}\left\{\frac{c_1\wp'(a, g_2, g_3) - \eta_1}{c_1\wp(a, g_2, g_3) - \eta_0 + c_2}\right\}^2 - c_1\wp(a, g_2, g_3) + 2c_2 - 2\eta_0 = 0,$$

which determines the phase shift L_0.

On the other hand, when $x \geq a/2$, the SPSWS can be expressed by

$$\eta(x) = -\frac{3\lambda}{2\alpha}\operatorname{sech}^2\sqrt{\frac{-\lambda}{4\beta}}(x - L_1),$$

where the phase shift L_1 is to be determined by the continuity conditions (23)–(24).

Consequently, for each solution L_0 of (30), we are able to construct an SPSWS to the BVP (8)–(9), which is expressed by

$$(31)\quad \eta(x) = \begin{cases} -\frac{3\lambda}{2\alpha}\operatorname{sech}^2\sqrt{\frac{-\lambda}{4\beta}}(x - L_0), & -\infty < x \leq -a/2, \\ c_1\wp(x+\tau, g_2, g_3) + c_2, & -a/2 < x < a/2, \\ -\frac{3\lambda}{2\alpha}\operatorname{sech}^2\sqrt{\frac{-\lambda}{4\beta}}(x - L_1), & a/2 \leq x < \infty. \end{cases}$$

4.2. Existence of multiple SPSWS. A salient feature of the BVP (8)–(9) with a well-shape forcing is that it may admit indefinitely large number of SPSWS for suitable parameters α and β, and sufficiently large values λ and a. We have numerically found that the number of the SPSWS of the BVP (8)–(9) is an increasing function of λ and the dent length a. In fact, (30) may define L_0 as a multivalued function of λ. For a given λ, the number of the corresponding solutions of L_0 to (30) is equal to the number of SPSWS of the BVP (8)–(9). Thus, the contour plot of $z = B(\lambda, L_0)$ at level zero reveals the bifurcation behavior of the solutions to the BVP (8)–(9).

To illustrate our numerical results, let us take $\alpha = -3/4$, $\beta = -1/6$, and a as a parameter. When $a = 1$, the contour plot (Fig. 2) of $z = B(\lambda, L_0)$ at level zero shows that there exist at most two solutions to (30) for $0 < \lambda \leq 4$. Precisely, there are no solution, one solution, and two solutions for $\lambda < \lambda_C (\approx 0.9916)$, $\lambda = \lambda_C$, and $\lambda_C < \lambda \leq 4$, respectively. This λ_C is called the turning point of the SPSWS bifurcation. Figure 3 (a) shows that there are four solutions to (30) for sufficiently large $\lambda > \lambda_{C_2}$ when $a = 2$. There are two turning points in this case. One is $\lambda_{C_1} (\approx 0.22175)$ and the other is $\lambda_{C_2} (\approx 0.339)$. Also, our numerical result demonstrates that there exists a pitchfork bifurcation at the turning point λ_{C_2}. Figure 3 (b) displays the local bifurcation diagram in the neighborhood of the two turning points. The gaps in Figs. 3 (a)–(b) are due to numerical errors. Moreover, we have found that there exist eight solutions to the BVP (8)–(9) when $a = 8$. In the case of $a = 8$, there are four turning points: $\lambda_{C_1} (\approx 0.3132)$, $\lambda_{C_2} (\approx 0.3395)$, $\lambda_{C_3} (\approx 1.3866)$, and $\lambda_{C_4} (\approx 2.2545)$. Figure 4 (a) shows the bifurcation diagram for $0 < \lambda \leq 4$, and Fig. 4 (b) shows the local bifurcation diagram for $0.3 < \lambda < 0.4$. Our numerical results have clearly

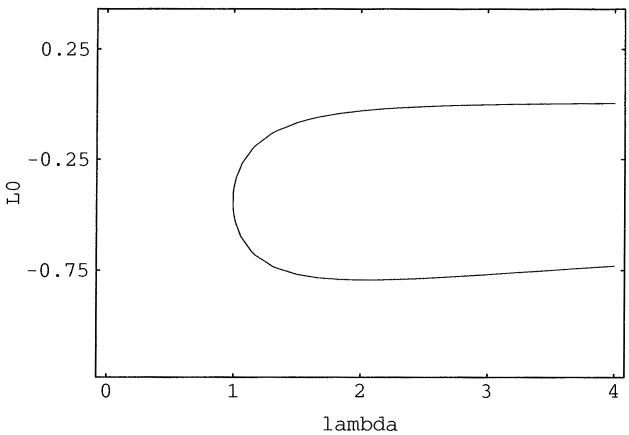

FIG. 2. *Bifurcation diagram of the* SPSWS *in the plane* (λ, L_0) *for* $a = 1$ *determined by the contour plot of* $z = B(\lambda, L_0)$ *at level zero.*

demonstrated the existence of two pitchfork bifurcations at the turning point λ_{C_2} (Fig. 4 (b)) and λ_{C_4} (Fig. 4 (a)). Another interesting feature is that there may exist nonsymmetric solutions in response to symmetric forcing and the nonsymmetric solutions must occur in pairs. In fact, for a symmetric forcing, $\eta(-x)$ is also an SPSWS if $\eta(x)$ is an SPSWS. Hence, the number of nonsymmetric solutions must be even. Figures 5 (a)–(b) show the graphs of two symmetric SPSWS and two nonsymmetric SPSWS when $a = 2$ and $\lambda = 3$, respectively. These two nonsymmetric SPSWS are indeed antisymmetric.

5. Numerical SPSWS. In §4, we have analytically solved the BVP (8)–(9) with a rectangular dent forcing function. But, the BVP (8)–(9), in general, cannot be solved analytically. It appears that it is not a trivial work to find multiple solutions numerically. Shen developed an efficient scheme which has proved to be applicable to any piecewise continuous forcing function in C_0^1 [8]. In this section, our objective is to use Shen's scheme to search for multiple numerical solutions for different forcings, for which analytic expressions of solutions cannot be found.

In order to make the numerical method and results self-contained here, we briefly describe Shen's numerical scheme in the first subsection before presenting the numerical results in the later subsections. The well-shape forcing function is reconsidered in the second subsection. The numerical results obtained here coincide with the analytic results obtained in §4. A partly negative and partly positive forcing function and two semi-elliptic bumps are taken as the forcing functions in the last two subsections, respectively.

5.1. Numerical scheme. Suppose that the forcing function vanishes outside the interval (x_-, x_+). For $x \leq x_-$, the solution of the BVP (8)–(9) is expressed by

$$\eta(x) = -\frac{3\lambda}{2\alpha}\operatorname{sech}^2\sqrt{\frac{-\lambda}{4\beta}}(x - L_0).$$

Here the phase shift L_0 is to be determined. We need to solve the BVP (8)–(9) for $x > x_-$. Different solutions are distinguished by different values of the phase shift L_0.

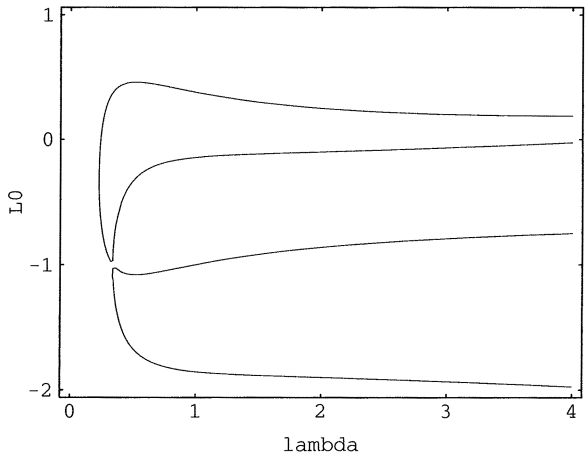

(a)

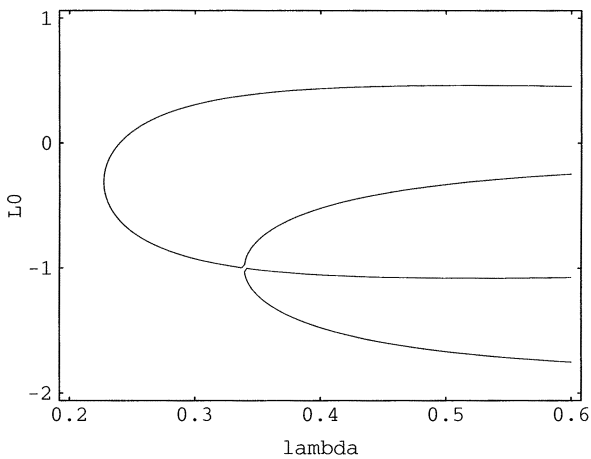

(b)

FIG. 3. (a) *Bifurcation diagram of the* SPSWS *in the plane* (λ, L_0) *for* $a = 2$ *determined by the contour plot of* $z = B(\lambda, L_0)$ *at level zero.* (b) *Local bifurcation diagram of the* SPSWS *in the plane* (λ, L_0) *for* $a = 2$ *near the two turning points.*

To determine L_0, we solve the following initial value problem:

$$\lambda\eta + \alpha\eta^2 + \beta\eta'' = f(x), \qquad x > x_-, \tag{32}$$

$$\eta(x_-) = -\frac{3\lambda}{2\alpha}\operatorname{sech}^2\sqrt{\frac{-\lambda}{4\beta}}(x_- - L_0), \tag{33}$$

$$\eta'(x_-) = -\sqrt{\frac{-\lambda}{\beta}}\eta(x_-)\tanh\sqrt{\frac{-\lambda}{4\beta}}(x_- - L_0) \tag{34}$$

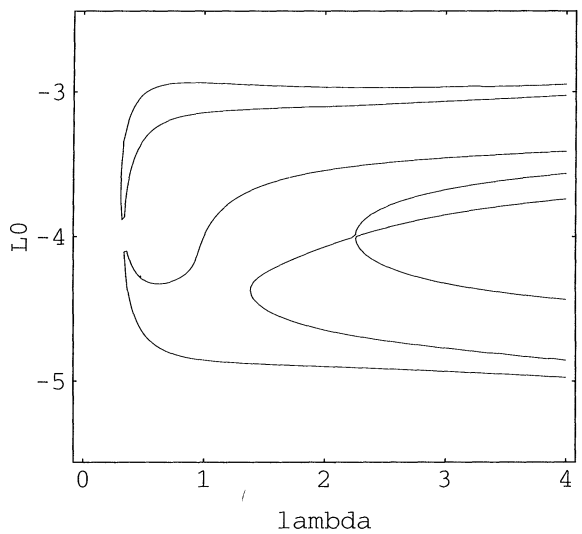

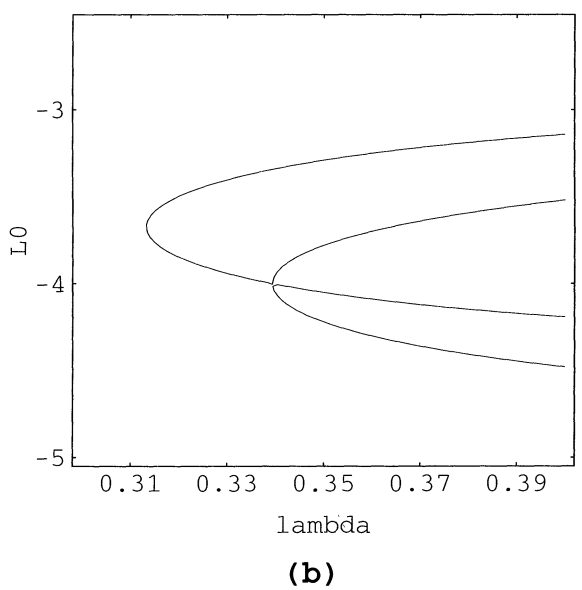

FIG. 4. (a) *Bifurcation diagram of the* SPSWS *in the plane* (λ, L_0) *for* $a = 8$ *determined by the contour plot of* $z = B(\lambda, L_0)$ *at level zero.* (b) *Local bifurcation diagram of the* SPSWS *in the plane* (λ, L_0) *for* $a = 8$ *near the first two turning points.*

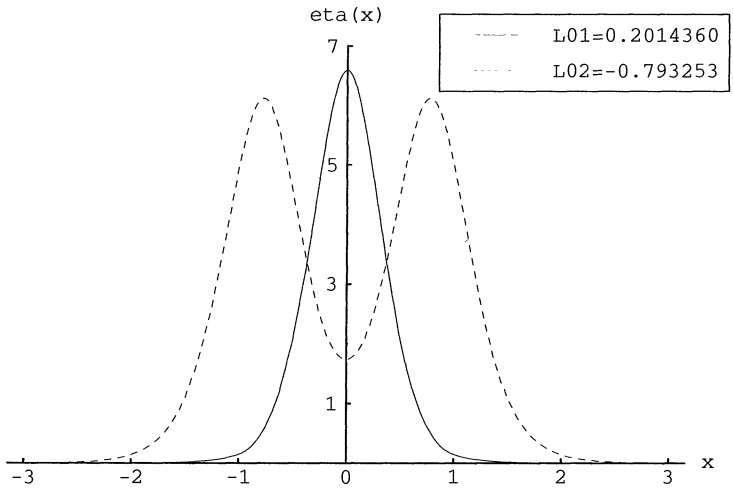

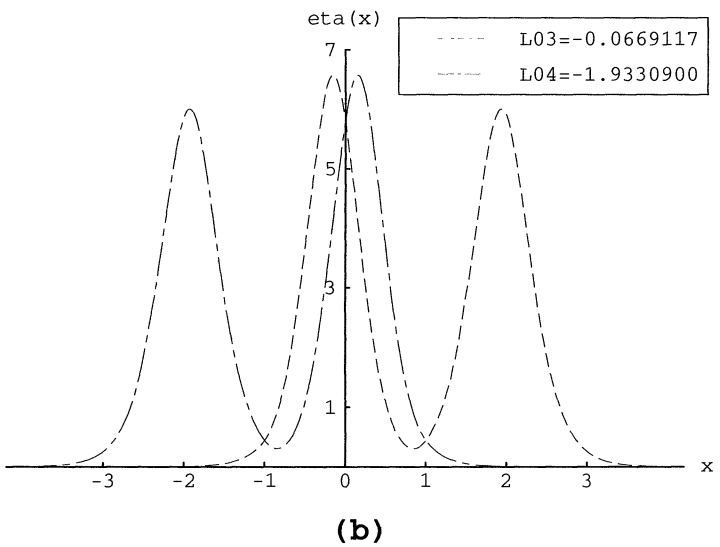

FIG. 5. (a) *Two symmetric solutions of the* sfKdV BVP *when* $a = 2$ *and* $\lambda = 3$ (*solid line,* $L_{01} = 0.201436$, *and dashed line,* $L_{02} = -0.793253$). (b) *Two nonsymmetric solutions of the* sfKdV BVP *when* $a = 2$ *and* $\lambda = 3$ (*dashed line,* $L_{03} = -0.0669117$, *and dot-dashed line,* $L_{04} = -1.93309$).

up to x_+ for a trial value of L_0, and compute

$$B_\lambda(L_0) \equiv \frac{\beta}{2}\left(\eta'(x_+)\right)^2 + \left(\frac{\lambda}{2} + \frac{\alpha}{3}\eta(x_+)\right)\eta^2(x_+).$$

The SPSWS $\eta(x)$ satisfies $\eta(+\infty) = 0$ if and only if $B_\lambda(L_0) = 0$ and $\eta(x_+) > 0$ for some L_0. If $|B_\lambda(L_0)| < 10^{-5}$, we consider this L_0 as a numerical approximation solution to $B_\lambda(L_0) = 0$. Using a do loop for L_0, a function $B_\lambda(L_0)$ versus L_0 can

be plotted in the $(L_0, B_\lambda(L_0))$ rectangular coordinate plane. The number of the intersections of the graph of the function $B_\lambda(L_0)$ with the L_0-axis is equal to the number of SPSWS of the BVP (8)–(9).

All computations were done on a SiliconGraphics workstation. The IVP (32)–(34) was solved by an ODE solver `NDSolve[ ]` in Mathematica. Numerical results for three types of forcing functions are reported below.

5.2. Well-shape forcing. Here, the well-shape forcing introduced in §4 is reconsidered. Figure 6 displays the curve of $B_\lambda(L_0)$ versus L_0 for $\lambda = 3$ in the case of $a = 2$. This curve has four intersection points with L_0-axis, i.e., $B_\lambda(L_0)$ has four zeros $L_0 = 0.201436$, -0.0669117, -0.793253, and -1.93309. Therefore, the BVP (8)–(9) has four SPSWS. These results coincide with those obtained from analytic solutions in §4 (see Fig. 3 (a)). All graphs of these solutions are shown in Figs. 5 (a)–(b).

5.3. Sine-shape forcing. In this section, the forcing we consider is defined by

$$f(x) = \begin{cases} \sin(\pi x), & -1 < x < 1, \\ 0, & \text{otherwise}, \end{cases}$$

which represents a partly positive bump and partly negative dent. The turning point of the bifurcation is $\lambda_C (\approx 1.391133)$. Namely, the BVP (8)–(9) has no solution, one solution, and two solutions for $\lambda < \lambda_C$, $\lambda = \lambda_C$, and $\lambda > \lambda_C$, respectively. The corresponding bifurcation diagram of the solutions in the $(\lambda, \eta(x_-))$ coordinates is shown in Fig. 7 (a). Figure 7 (b) shows the $B_\lambda(L_0)$ curves when λ=3.3, 1.391133 and 1.1, respectively. When $\lambda = 1.1$, $B_\lambda(L_0)$ has no zero, which implies that the BVP (8)–(9) has no solution. When $\lambda = \lambda_C$, $B_\lambda(L_0)$ has only one zero, $L_0 = -1.003546$. Hence, the BVP (8)–(9) has only one SPSWS (Fig. 7 (c)). When $\lambda = 3.3$, $B_\lambda(L_0)$ has two zeros: $L_{01} = -1.1791328$ and $L_{02} = -0.5662725$. Hence, the BVP (8)–(9) has two SPSWS (Fig. 7 (d)).

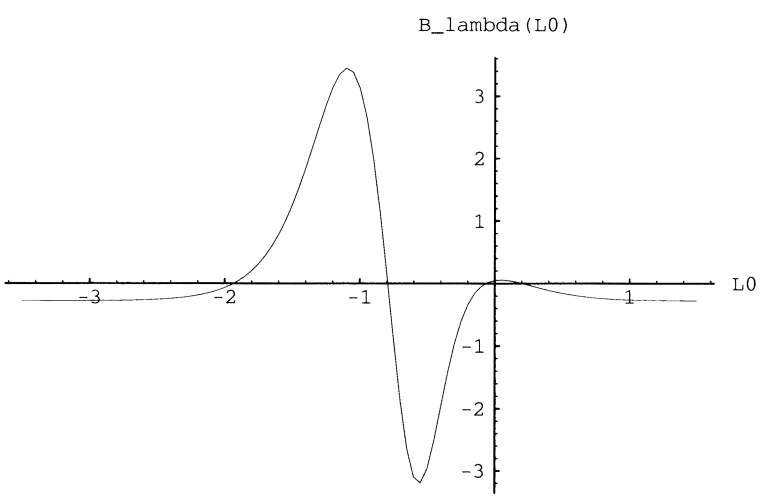

FIG. 6. $B_\lambda(L_0)$ *curve versus* L_0 *when* $\lambda = 3$ *and* $a = 2$ *described in* §5.2.

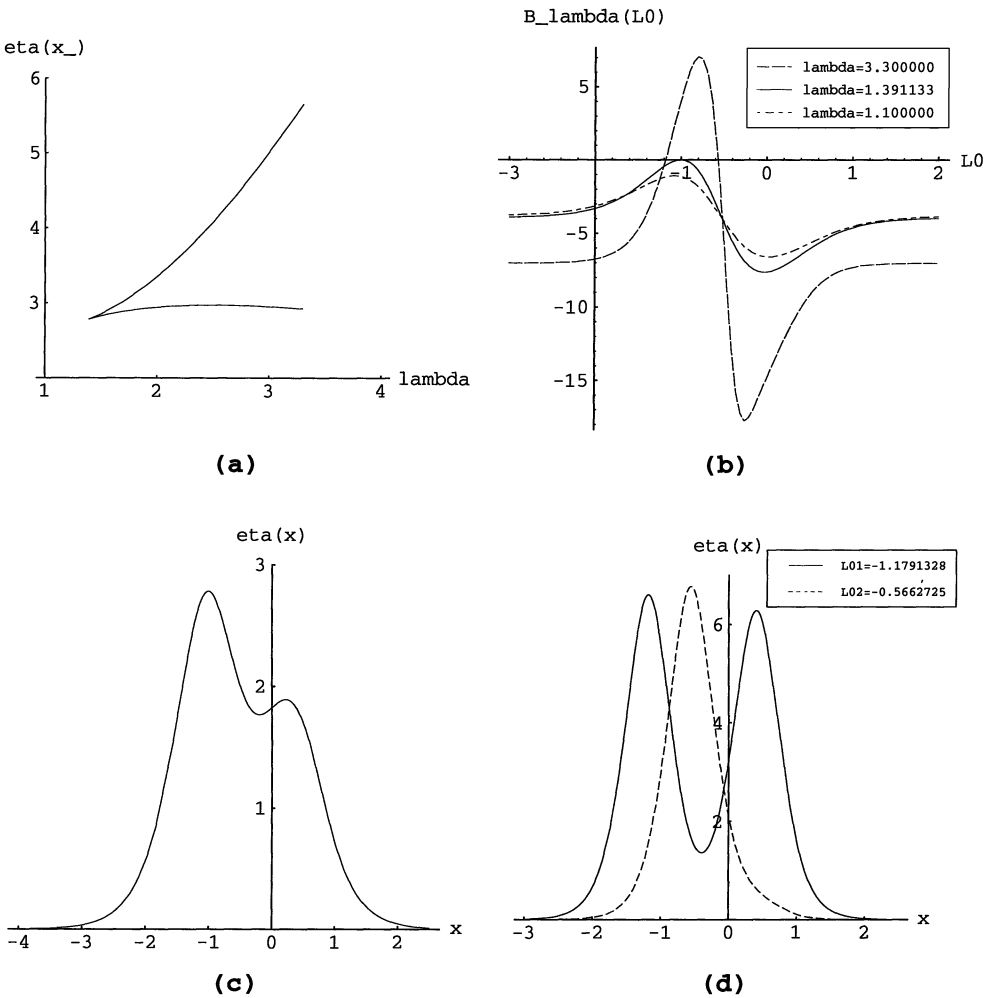

FIG. 7. (a) *Bifurcation diagram of the* sfKdV BVP *in the plane* $(\lambda, \eta(x_-))$ *described in section* 5.3. (b) $B_\lambda(L_0)$ *curves versus* L_0 *described in* §5.3, *when* $\lambda = 1.1$ (*no intersection point with the* L_0-*axis*), $\lambda = 1.391133$ (*one intersection point with the* L_0-*axis*), *and* $\lambda = 3.3$ (*two intersection points with the* L_0-*axis*). (c) *The solution of the* sfKdV BVP *when* $\lambda = 1.391133$ ($L_0 = -1.003546$). (d) *Two solutions of the* sfKdV BVP *when* $\lambda = 3.3$ (*solid line,* $L_{01} = -1.1791328$, *and dashed line,* $L_{02} = -0.5662725$).

5.4. Two semi-elliptic bump forcing. In this section, the forcing we consider is defined by

$$f(x) = \begin{cases} \frac{1}{2}\sqrt{1-(x+2)^2}, & |x+2| < 1, \\ \frac{1}{2}\sqrt{1-(x-2)^2}, & |x-2| < 1, \\ 0, & \text{otherwise}, \end{cases}$$

which represents two positive semi-elliptic bumps. In this case, we find that the crucial value λ_C is close to 0.94329. Thus, when $\lambda < \lambda_C$, the BVP (8)–(9) has no solution. When $\lambda = \lambda_C$, the BVP (8)–(9) has only one solution (Fig. 8 (a)) since $B_\lambda(L_0)$ has

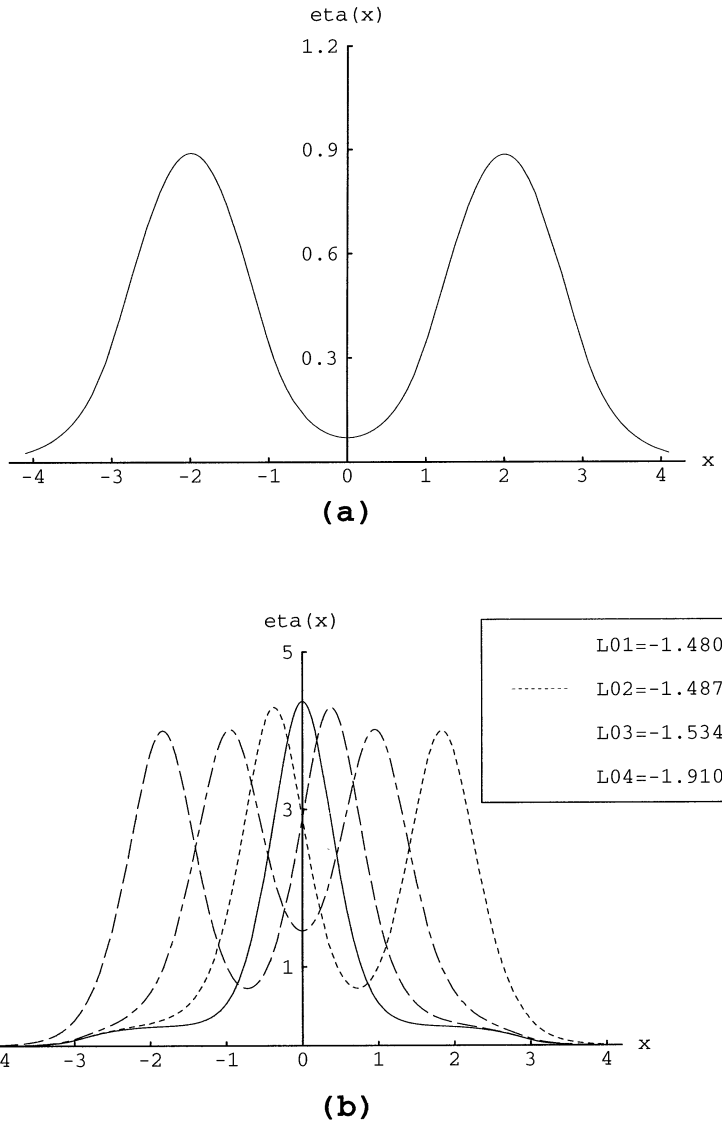

FIG. 8. (a) *The solution of the* sfKdV BVP *when* $\lambda = 0.9433$ ($L_0 = -1.7329$) *described in* §5.4. (b) *Four solutions of the* sfKdV BVP *when* $\lambda = 2.2$ *described in* §5.4.

only one zero at $L_0 = -1.732782$. When $\lambda > \lambda_C$, the BVP (8)–(9) has more than one solution. For instance, when $\lambda = 2.2$, $B_\lambda(L_0)$ has four zeros: $L_{01} = -1.480978$, $L_{02} = -1.487165$, $L_{03} = -1.534397$, and $L_{04} = -1.910591$. Figure 8 (b) displays these four solutions: two symmetric ($L_{01} = -1.480978$ and $L_{03} = -1.534397$) and two nonsymmetric ($L_{02} = -1.487165$ and $L_{04} = -1.910591$). It is clear that two nonsymmetric solutions are antisymmetric.

6. Stability of the SPSWS. We have analytically and numerically demonstrated that there are many branches of SPSWS to the BVP (8)–(9). A natural and important question is which solution is stable with respect to the time dependent

fKdV equation

$$\eta_t + \lambda\eta_x + 2\alpha\eta\eta_x + \beta\eta_{xxx} = f_x, \quad -\infty < x < \infty, \tag{35}$$

$$\eta(x, t = 0) = \eta_s(x), \qquad \eta(\pm\infty, t) = 0, \tag{36}$$

where $\eta_s(x)$ is a stationary SPSWS of the sfKdV BVP (8)–(9).

This stability problem is numerically investigated in this section. The instability of the SPSWS may be loosely described in the following way. We numerically solve the IVP (35)–(36) up to a certain time t. Naturally, the small perturbation due to the truncation error in the numerical computation is introduced to the system. If the initial profile is subject to a dramatical change in a short time (say, $t \leq 30$), then we say that this stationary solution $\eta_s(x)$ is unstable. It is also noticed that the wave resistance coefficient

$$C_{D_w}(t) \equiv -\int_{-\infty}^{+\infty} f\eta_x dx = \frac{1}{2}\frac{d}{dt}\int_{-\infty}^{+\infty} \eta^2 dx, \tag{37}$$

introduced by Wu [13], characterizes the rate of the change of the momentum of the wave evolution. This quantity can be used to discern the stability of an SPSWS as well. Namely, the stationary solution $\eta_s(x)$ is said to be unstable if the wave resistance coefficient $C_{D_w}(t)$ varies in time. Otherwise, it is stable.

For numerical simulations, the psuedo-spectral scheme developed by Chan and Kerkhoven [3] are extended to solve the IVP (35)–(36). In this scheme, the infinite domain in space is replaced by $-L < x < L$ with L sufficiently large and the periodic boundary condition $\eta(-L, t) = \eta(L, t)$ for any time $t > 0$ is used. We carried out numerical simulations for the case of the well-shape forcing introduced in §4. As discussed earlier, the BVP (8)–(9) with the dent length $a = 2$ admits four SPSWS when $\lambda = 3$. All numerical results are presented in Figs. 9–12 where (a) always shows the evolution of the initial wave profile and (b) manifests the wave resistance coefficient $C_{D_w}(t)$. For a well-shape forcing, the wave resistance coefficient $C_{D_w}(t)$ is simply written as

$$C_{D_w}(t) = \eta(a/2, t) - \eta(-a/2, t). \tag{38}$$

Our numerical results suggest that only one SPSWS is stable and all the others are unstable.

Let us explain the numerical results as follows. Figure 9 (a) exhibits the evolution of a symmetric SPSWS (solid line in Fig. 5 (a)). One can see that the initial wave profile remains in the same form up to time $t = 30$. Also, Fig. 9 (b) demonstrates that the curve of the wave resistance coefficient $C_{D_w}(t)$ is fairly flat. Thus, this SPSWS is stable. Two nonsymmetric SPSWS are obviously unstable (Figs. 10-11). Figure 10 (a) shows that the higher amplitude wave evolves into the stable steady-state while the lower amplitude wave deforms a little and propagates away from the initial state. This result provides evidence of the existence of "the basin of attraction" in the system. The terminology "the basin of attraction" is adopted from Camassa and Wu's paper [2]. The other symmetric SPSWS is unstable as well. Figure 12 (a) shows that the wave profiles shift left and right slightly around the initial profile and (b) shows the oscillation of the wave resistance coefficient $C_{D_w}(t)$.

Throughout our numerical computation, we have taken $L = 32$ and the number of the collocation points $N = 512$. Due to the requirement for the linear stability of the

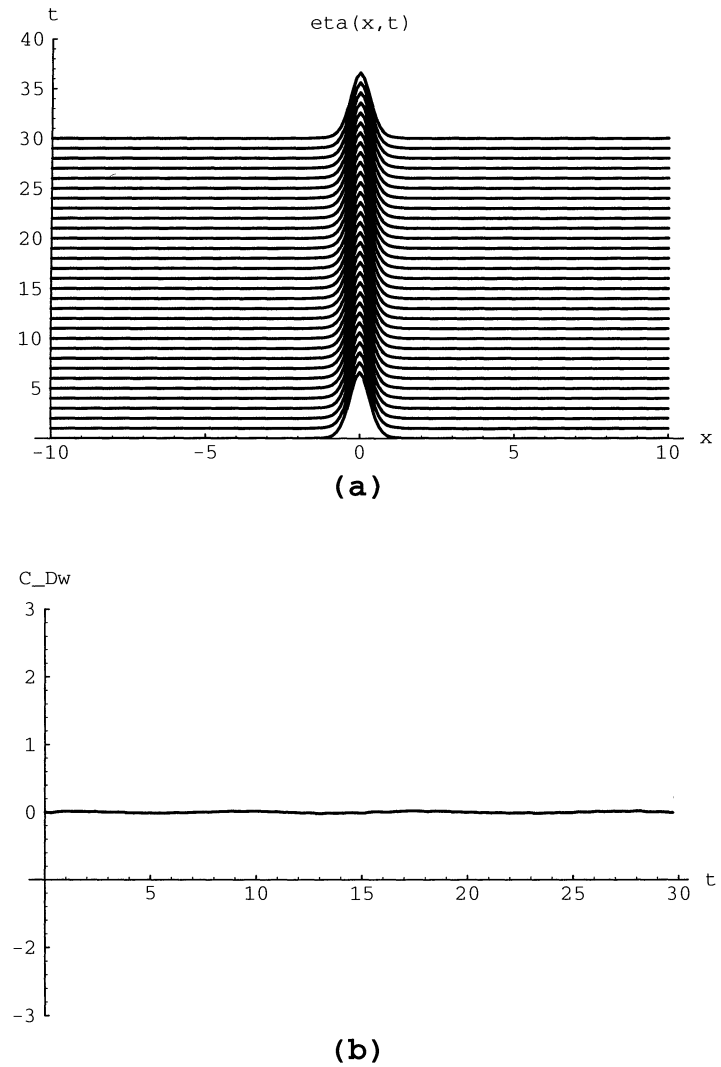

FIG. 9. (a) *Evolution of the stable* SPSWS, *corresponding to the solid line in Fig.* 5 (a), *when* $a = 2$. (b) *The wave resistance coefficient* $C_{D_w}(t)$ *versus* t.

scheme (cf. [3]), the time step Δt is taken as 0.005. All numerical computations are implemented by a Mathematica code called "srecfkdv.m" on a SiliconGraphics workstation. For the purpose of viewing the main characteristics of the wave motion, Figs. 9–12 (a) only display the evolution of wave profiles in a subinterval of $(-L, L)$.

7. Concluding remarks. We have studied the supercritical positive solitary wave solutions (SPSWS) of the stationary forced Korteweg–de Vries equation (sfKdV) and their stability when the forcing is nonlocal. Here, a "nonlocal forcing" means that the support of the forcing in the physical problem is of comparable length with the length scale L of the free surface wave. Hence, each type of forcing considered here has a long support. In summary, we have analytically and numerically demonstrated that

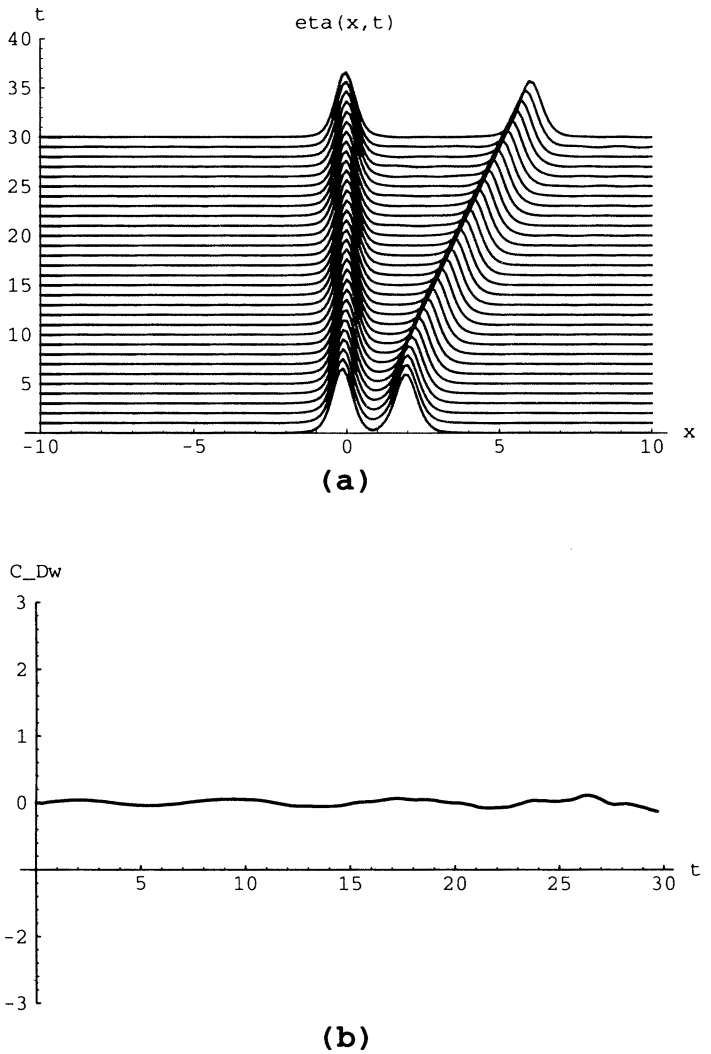

FIG. 10. (a) *Evolution of the unstable* SPSWS, *corresponding to the dashed line in Fig.* 5 (b), *when* $a = 2$. (b) *The wave resistance coefficient* $C_{D_w}(t)$ *versus* t.

the stationary forced KdV equation can have more than two SPSWS for a nonlocal forcing. There may exist $2N$ SPSWS for an arbitrary integer N when a and λ are sufficiently large in the case of the well-shape forcing. At the turning points from two SPSWS to four SPSWS, from four solutions to six solutions, and so on, there may exist pitchfork bifurcations. Nonsymmetric solutions exist in response to the symmetric forcing. They must occur in pairs.

It is worth remarking that Camassa and Wu have recently investigated the stability of the forced sech^2-like solitary waves [1]–[2]. They analyzed the linear instability of the stationary forced solitary waves due to infinitesimal disturbances. Three different categories of the stationary forced solitary waves are identified, which occur in three different parametric régimes called a periodic bifurcating régime, an aperiodic bifurcating régime, and a supercritical stable régime. They also did nonlinear

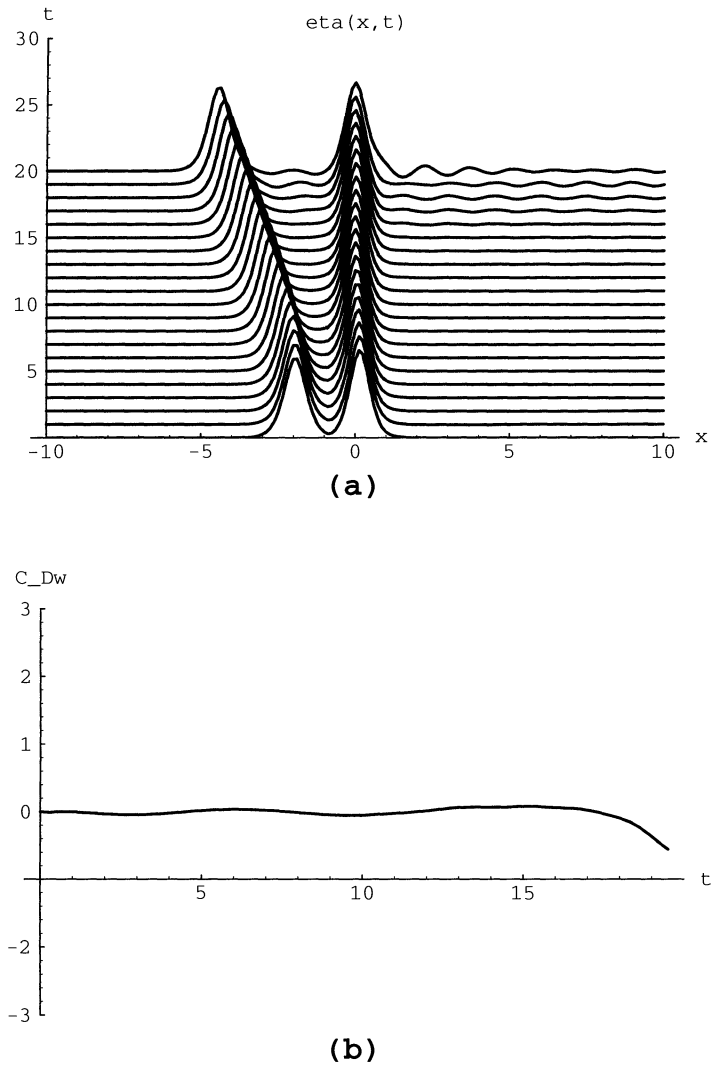

FIG. 11. (a) *Evolution of the unstable* SPSWS, *corresponding to the dot-dashed line in Fig.* 5 (b), *when* $a = 2$. (b) *The wave resistance coefficient* $C_{D_w}(t)$ *versus* t.

stability analysis from the Hamiltonian functional formulation. In general, it is very difficult to analyze the stability of the stationary forced solitary waves. Even if analytic expression of SPSWS to the sfKdV equation is found for a nonlocally negative forcing described in §4, the structure of the SPSWS is still complicated. Numerical simulations reported in §6 suggest that only one SPSWS is stable and the others are unstable. To the authors' knowledge, there have not been experiments conducted for nonlocally forced cases. It seems that a further experimental study on this stability problem will be worthwhile.

Acknowledgments. We thank Professor T.Y. Wu of the California Institute of Technology and Dr. R. Camassa of the Los Alamos National Laboratory for their helpful suggestions and conversations that led us to make use of the wave resistance

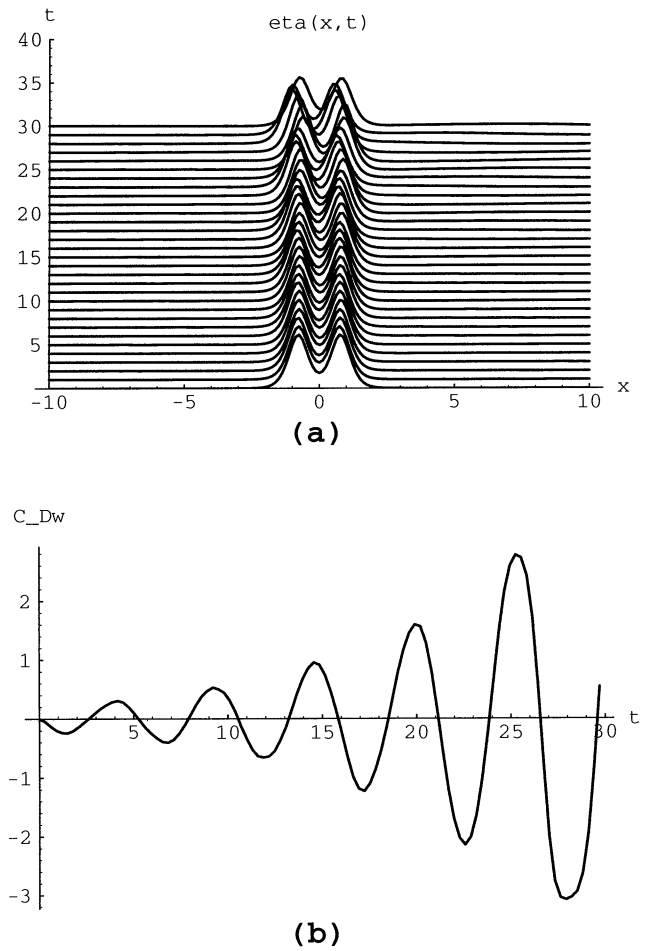

FIG. 12. (a) *Evolution of the unstable* SPSWS, *corresponding to the dashed line in Fig.* 5 (a), *when* $a = 2$. (b) *The wave resistance coefficient* $C_{D_w}(t)$ *versus* t.

coefficient for discerning the instability of the SPSWS. We also thank Dr. J.J. Morgan for many interesting discussions on multiple solitary wave solutions.

REFERENCES

[1] R. CAMASSA AND T. YAO-TSU WU, *Stability of forced solitary waves*, Phil. Trans. R. Soc. Lond. A, 337 (1991), pp. 429–466.

[2] ———, *Stability of some stationary solutions for the forced* KdV *equation*, Physica D, 51 (1991), pp. 295–307.

[3] T. F. CHAN AND T. KERKHOVEN, *Fourier methods with extended stability intervals for the Korteweg–de Vries equation*, SIAM J. Numer. Anal., 22 (1985) pp. 441–454.

[4] L. K. FORBES AND L. W. SCHWARTZ, *Free-surface flow over a semi-circular obstruction*, J. Fluid Mech., 114 (1982), pp. 299–314.

[5] D. LUDWIG, *Parsimonious asymptotics*, SIAM J. Appl. Math., 43 (1983), pp. 664–672.

[6] A. PATOINE AND T. WARN, *The interaction of long, quasi-stationary baroclinic waves with topography*, J. Atoms. Sci., 39 (1982), pp. 1018–1025.

[7] A. S. PETERS AND J. J. STOKER, *Solitary waves in liquids having non-constan density*, Comm. Pure Appl. Math., 13 (1960), pp. 115–164.

[8] S. S. P. SHEN, *Disturbed critical surface waves in a channel of arbitrary cross section*, J. Appl. Math. Phys. (ZAMP), 40 (1989), pp. 216–229.
[9] S. S. P. SHEN, *Locally forced critical surface waves in channels of arbitrary cross section*, J. Appl. Math. Phys. (ZAMP), 42 (1991), pp. 122–138.
[10] S. S. P. SHEN, *Forced solitary waves and hydraulic falls in two-layer flows*, J. Fluid Mech., 234 (1992), pp. 583–612.
[11] J. -M. VANDEN-BROECK, *Free-surface flow over a semi-circular obstruction in a channel*, Phys. Fluids, 30 (1987), pp. 2315–2317.
[12] Z. X. WANG AND D. R. GUO, *Special Functions*, World Scientific, Singapore, 1989.
[13] T. Y. WU, *On generation of solitary waves by moving disturbances*, J. Fluid Mech., 184 (1987), pp. 75–99.